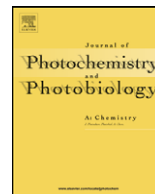




Contents lists available at ScienceDirect

# Journal of Photochemistry and Photobiology A: Chemistry

journal homepage: [www.elsevier.com/locate/jphotochem](http://www.elsevier.com/locate/jphotochem)

## The excited states interaction of safranin-O with PAMAM and DAB dendrimers in methanol

Carlos A. Suchetti, Ana I. Novaira, Sonia G. Bertolotti, Carlos M. Previtali\*

Departamento de Química, Universidad Nacional de Río Cuarto, 5800 Río Cuarto, Argentina

### ARTICLE INFO

#### Article history:

Received 4 September 2008

Accepted 26 September 2008

Available online 21 October 2008

#### Keywords:

Triplet quenching  
Safranin  
Dendrimers  
PAMAM  
DAB

### ABSTRACT

The quenching of the excited singlet and triplet states of the synthetic dye safranin-O by low generation PAMAM and DAB dendrimers was investigated in methanol. The rate constants for the quenching of the excited singlet state depend on the number of primary amino groups in the dendrimer. The first-order rate constant for the decay of the triplet state presents a downward curvature as a function of the quencher concentration. This behavior was interpreted in terms of the reversible formation of an intermediate complex in the excited state. From a kinetic analysis of the quenching mechanism the equilibrium constant  $K_{exc}$  could be extracted. The values of  $K_{exc}$  may be related to the proton affinity of the quencher. The results were interpreted in terms of a reversible proton transfer quenching. This was further confirmed by the transient absorption spectra obtained by laser flash photolysis. The transient absorption immediately after the triplet state quenching could be assigned to the unprotonated form of the dye. At later times the spectrum matches the semireduced form of the dye. The overall process corresponds to a one-electron reduction of the dye mediated by the deprotonated triplet state.

© 2008 Elsevier B.V. All rights reserved.

### 1. Introduction

Dendrimers are molecules characterized by a highly branched compact structure of great regularity and they may contain a large number of reactive end groups. Their applications range from drug delivery [1] to molecular encapsulation and gene therapy [2] and building blocks for nanostructures [3]. Dendrimers of lower generations (0, 1, and 2) have highly asymmetric shape and possess more open structures as compared to higher generation dendrimers. As the chains growing from the core molecule become longer and more branched, dendrimers adopt a globular structure and they are frequently described as unimolecular micelles. Among the most commonly used dendrimers are poly(propyleneimine) (PPI) and poly(amidoamine) (PAMAM) dendrimers. PPI dendrimers are also denoted DAB-dendrimers where DAB refers to the diaminobutane core structure.

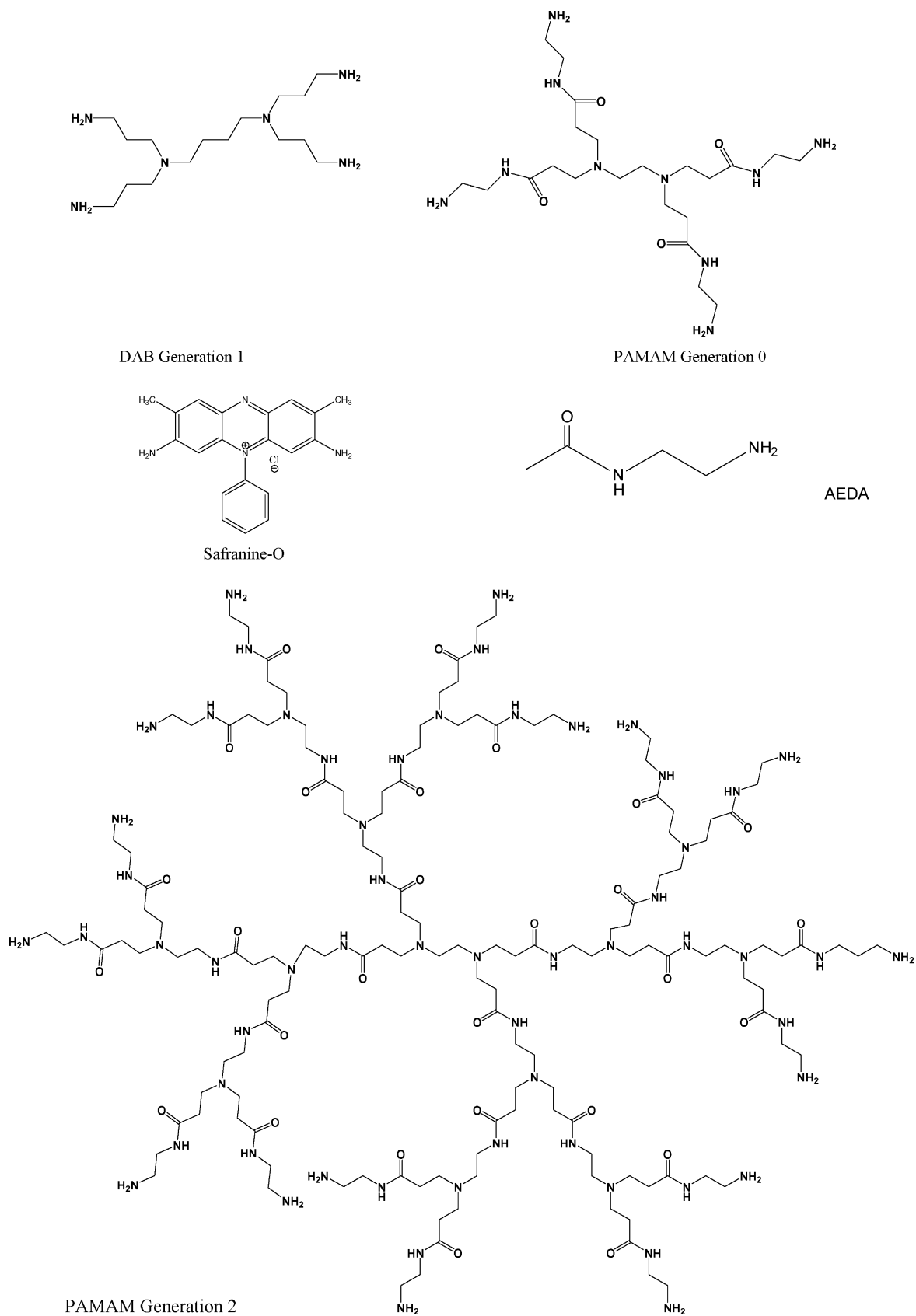
Recently, the use of PPI dendrimers as co-initiators in photoinitiated radical polymerization, has been tested [4]. The photopolymerization was carried out with UV radiation employing benzophenone and thioxanthone as sensitizers. The investigation of the structure of the resulting polymers suggested the presence of stretched polymer chains around the dendrimer. In another study, macrophotoinitiators were prepared using DAB

dendrimers and thioxanthone as sensitizer in the UV [5]. These initiators were found suitable for use in aqueous systems. The use of dendrimers as co-initiators seems to be promising and it was therefore of interest to investigate the extension of their use to the visible zone of the spectrum. We have previously investigated several photoinitiating systems operating in the visible region. In particular the synthetic dye safranin-O, which absorbs around 500 nm, was used as sensitizer and several aliphatic amines were employed as co-initiators (hydrogen donors) [6]. This system was found to be highly efficient for the free radical polymerization of vinyl monomers. The system was also shown to be useful for photopolymerization in aqueous media [7] and the addition of a third component (diphenyliodonium salt) improved the efficiency of the system safranin-triethanolamine in aqueous photopolymerization of acrylamide [8]. The deactivation mechanism of the excited states of safranin, and the related dye phenosafranin, in the presence of aliphatic and aromatic amines have been the subject of several studies of our group [9–11]. Therefore, it was of interest to explore the possibility of using dendrimers as co-initiators with safranin-O as sensitizer.

In this paper we present the investigation of the excited states interactions of safranin-O with low generation dendrimers containing amino terminal groups. The effect of the dendrimer structure on the reactivity of excited singlet and triplet states is investigated by static and time-resolved spectroscopies. It is found that a proton transfer process is the initial reaction in the case of the

\* Corresponding author.

E-mail address: [cprevitali@exa.unrc.edu.ar](mailto:cprevitali@exa.unrc.edu.ar) (C.M. Previtali).



Scheme 1.

triplet state, while an electron transfer process is the deactivation process in the case of the excited singlet.

The structures of the dye and quenchers are shown in Scheme 1.

## 2. Experimental

### 2.1. Materials

Safranin-O ( $\text{SfH}^+\text{Cl}^-$ ) was purchased from Aldrich and was used without further purification. It was checked that its photophysical properties coincided with those reported in the literature. The dendrimers were also from Aldrich and were obtained as methanolic solution in the case of PAMAM generation 0 (PAMAM-G0) and generation 2 (PAMAM-G2), and in the pure form (liquid) in the case of PPI-diaminobutane, generation 1 (DAB-G1). Triethylamine (TEA), n-butylamine (BA) and triethanolamine (TEOHA) (Aldrich) were purified by vacuum distillation. N-Acetyl-ethylenediamine (AEDA) from Aldrich was purified by sublimation. Methanol, HPLC grade, was from Merck or Sintorgan.

### 3. Measurements

Absorption spectra were recorded using a HP8453 diode array spectrophotometer. Steady-state fluorescence experiments were carried out with a Spex Fluorolog spectrofluorometer. Fluorescence lifetime measurements were done with the time correlated single photon counting technique using Edinburgh Instruments OB-900 equipment. The fluorescence determinations were carried out with air-equilibrated solutions. Transient absorption spectra and triplet quenching were determined by laser flash photolysis. A Spectron SL400 Nd:YAG laser generating 532 nm laser pulses (20 mJ per pulse, ca. 18 ns FWHM) was the excitation source. The laser beam was defocused in order to cover all the path length (10 mm) of the analyzing beam from a 150-W Xe lamp. The experiments were performed with rectangular quartz cells with right angle geometry. The detection system comprises a PT1 monochromator coupled to a Hamamatsu R666 PM tube. The signal was acquired by a digitizing scope (Hewlett-Packard 54504) where it was averaged and then transferred to a computer. All the kinetic determinations were performed at  $20 \pm 1^\circ\text{C}$ . For the laser photolysis experiments the solutions were de-oxygenated by bubbling during 30 min with solvent saturated high purity argon.

## 4. Results and discussion

### 4.1. Singlet state quenching

The visible absorption spectrum of  $\text{SfH}^+$  in MeOH consists of a strong band at 529 nm. The spectrum did not show any change in the presence of aliphatic amines or PAMAM and DAB dendrimers, thus ground-state interactions can be disregarded. The fluorescence emission maximum is at 564 nm. It was quenched by PAMAM and DAB without changes of the spectral shape.

Fluorescence lifetimes were determined in the absence and the presence of the quenchers. The lifetime of  $\text{SfH}^+$  excited singlet was  $2.60 \pm 0.05$  ns at room temperature ( $20^\circ\text{C}$ ) in air-equilibrated methanolic solution. Fig. 1 shows the reciprocal of the fluorescence lifetime as a function of the quencher concentration. From these plots bimolecular quenching rate constants were determined according to the following equation:

$$\tau^{-1} = \tau_0^{-1} + {}^1k_q[Q] \quad (1)$$

where  $\tau_0$  and  $\tau$  stand for the fluorescence lifetime in the absence and the presence of the quencher  $Q$ , respectively.

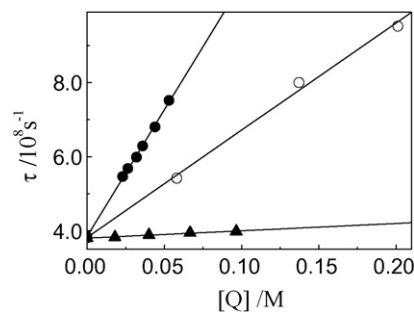


Fig. 1. Dynamic quenching of  $\text{SfH}^+$  fluorescence by dendrimers and n-butylamine in air-equilibrated methanolic solutions. (●) PAMAM-G2, (○) DAB, (▲) BA.

The quenching was investigated for three low generation dendrimers: PAMAM-G0, PAMAM-G2 and DAB-G1 and several aliphatic amines: BA, TEA, TEOHA and AEDA. The rate constants are collected in Table 1. It can be seen that the primary amines BA and AEDA are the less efficient quenchers while TEOHA is the more effective. PAMAM-G0, in spite of having two tertiary nitrogen atoms and four amino terminal groups, quenches with a rate constant similar to that of TEA. PAMAM-G2 has a rate constant that is only five times larger than that of G0. This factor is close to the ratio of terminal amino groups between PAMAM-G2 (16 groups) and PAMAM-G0 (4 groups). This means that the inner tertiary amino groups do not have an important contribution to the quenching. Moreover, when compare with BA the reactivity of both PAMAM dendrimers keeps a close relationship with the number of external primary amino groups.

It was previously demonstrated that singlet quenching of  $\text{SfH}^+$  by aliphatic amines takes place by an electron transfer mechanism [10]. Primary aliphatic amines have a higher oxidation potential than secondary or tertiary amines; therefore, they present a lower reactivity. Of the amines here employed, TEOHA has the lower oxidation potential and consequently the higher rate constant. The reactivity of PAMAM-G0 and -G2 may be understood in terms of two factors: first, the tertiary amino groups are imbedded in the dendritic structure, and second, the amide groups produce a deactivating effect of the electron donor capacity of the structure. The latter effect is more apparent by comparing DAB-G1 with PAMAM-G0. Both dendrimers have four terminal primary and two inner tertiary amino groups, however, DAB is twice as reactive as PAMAM-G0. The deactivating effect of the amide group is confirmed by the low quenching efficiency of the model compound AEDA.

### 4.2. Triplet state quenching

The T-T transient absorption of  $\text{SfH}^+$  in MeOH presents three main bands at 430, 735 and 820 nm. It decays in tens of microseconds, mainly by self-quenching, to the semireduced and semioxidized forms of the dye. The triplet state is efficiently quenched by aliphatic amines [10] and it decays with a first-order kinetics. The quenching by dendrimers and the amines was investigated by laser flash photolysis, following excitation of the dye at 532 nm. The kinetics of quenching was monitored by the decay of the absorption at 820 nm. In Fig. 2 the plots of the first-order rate constant as a function of the quencher concentration are shown. It can be seen that in all cases the plots present a downward curvature.

A similar effect was observed for the quenching of the related dye phenosafranin by aliphatic amines [12]. This downward curvature was ascribed to the occurrence of fast proton transfer equilibrium in the excited state. This is further corroborated by the transient absorption spectra determined by laser flash photolysis of  $\text{SfH}^+$  in the presence of the quenchers. In Fig. 3 the spectra in the

**Table 1**  
Rate constants for the quenching of the excited singlet and triplet states of safranine-O.

Quencher	Singlet		Triplet		
	$k_q$ ( $10^9 \text{ M}^{-1} \text{ s}^{-1}$ )		$k_d k_{exc}$ ( $10^9 \text{ M}^{-1} \text{ s}^{-1}$ )	$K_{exc}$ ( $\text{M}^{-1}$ )	$k_d$ ( $10^6 \text{ s}^{-1}$ )
BA	0.20		1.7	$1100 \pm 300$	1.1
PAMAM-G0	1.3		0.55	$600 \pm 200$	0.97
PAMAM-G2	6.8		3.2	$2300 \pm 200$	1.5
DAB-G1	2.9		6.1	$5600 \pm 1000$	1.09
TEA	1.3		0.8	$1700 \pm 500$	0.47
AEDA	0.23		0.38	$700 \pm 300$	0.51
TEOHA	4.1		0.0038 <sup>a</sup>		
N,N-dimethyl-aniline	12.0		5.2 <sup>a</sup>		

<sup>a</sup> Linear plot.

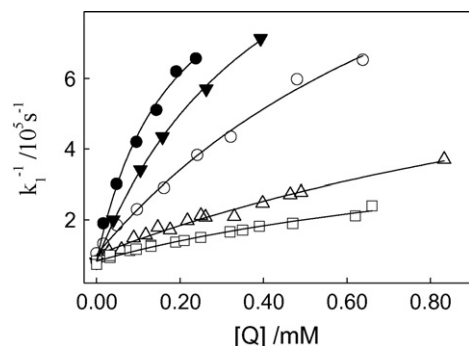


**Fig. 2.** First-order decay rate constant of  $^3\text{SfH}^+$  measured at 820 nm as a function of quencher concentration. (●) DAB, (▲) PAMAM-G2, (○) BA, (△) PAMAM-G0, (□) AEDA. Solid lines calculated according to Eq. (2).

presence of PAMAM-G0 at different times after the laser pulse are presented.

It can be seen that at the same time the absorption at 820 nm of the monoprotonated triplet  $^3\text{SfH}^+$  decays, a new absorption at 420 nm develops; afterwards it decays and at the same time a growth is apparent at 460 nm. These absorptions can be ascribed to the deprotonated triplet  $^3\text{Sf}$  ( $\lambda_{\text{max}}$  420 nm) and the semireduced form of the dye ( $\lambda_{\text{max}}$  440 nm). An enlargement of the changes in this region is presented in Fig. 4 and the time profiles of the absorption are shown in Fig. 5. It can be seen that the absorption at 410 nm grows at the same time that the 820 nm signal decays. Afterwards, the absorption at 410 nm (assigned to  $^3\text{Sf}$ ) decays and the semireduced form, absorbing at 460 nm, develops.

In Fig. 6 a comparison of the spectrum of the dye in the presence of NaOH 1 mM in MeOH and the spectrum in the presence of PAMAM-G0 taken at an intermediate time is presented. The spectrum with NaOH develops in less than 1  $\mu\text{s}$  and is practically

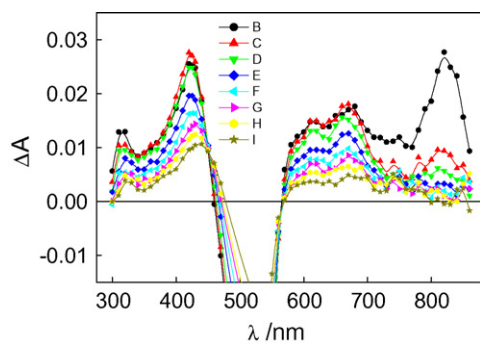


**Fig. 3.** Transient absorption spectra of  $\text{SfH}^+$  in the presence of PAMAM-G0 0.5 mM at different times. B = 2  $\mu\text{s}$ , C = 5  $\mu\text{s}$ , D = 10  $\mu\text{s}$ , E = 20  $\mu\text{s}$ , F = 30  $\mu\text{s}$ , G = 40  $\mu\text{s}$ , H = 50  $\mu\text{s}$ , and I = 70  $\mu\text{s}$ .

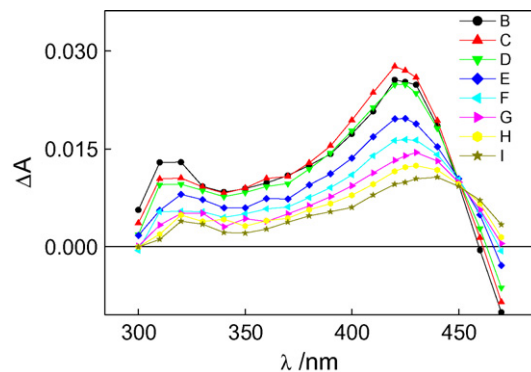


**Fig. 4.** Enlargement of the region 300–500 nm of Fig. 3. Same symbols as in Fig. 3.

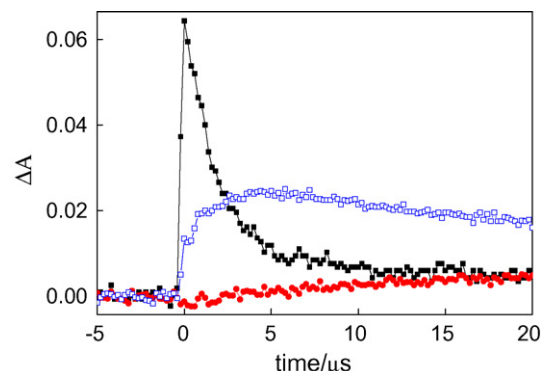


**Fig. 5.** Absorption profiles at 830 nm (black) 410 nm (blue) 460 nm (red) of  $\text{SfH}^+$  after laser flash irradiation in the presence of PAMAM-G0 0.5 mM. (For interpretation of the references to color in this figure legend, the reader is referred to the web version of the article.)

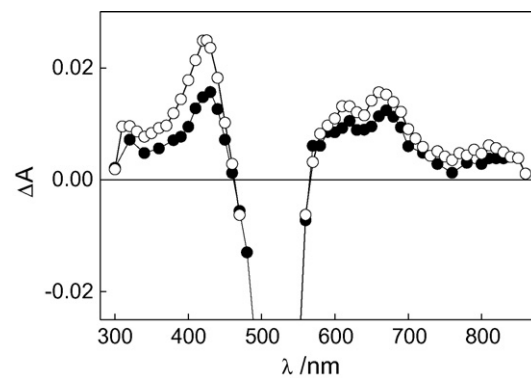
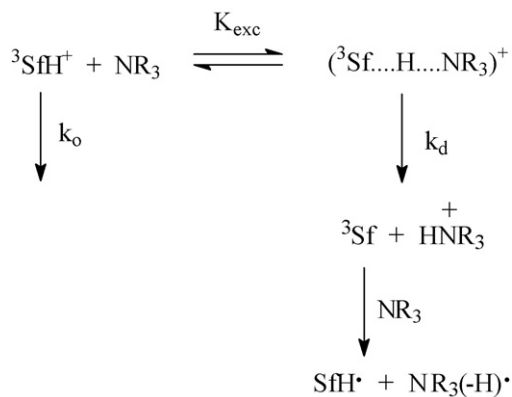


**Fig. 6.** Transient absorption spectrum of  $\text{SfH}^+$  in the presence of NaOH 1 mM at 2  $\mu\text{s}$  after the laser pulse (●) and in the presence of PAMAM-G0 0.5 mM at 10  $\mu\text{s}$  after the laser pulse (○).



Scheme 2.

undistinguishable from the spectrum in the presence of PAMAM-GO taken at 5  $\mu\text{s}$ .

This is a confirmation that the initial step in the triplet quenching of the dye by the dendrimer is a deprotonation reaction. At longer times an absorption band in the region 600–700 nm initially present, decays slowly in several tens of microseconds. In this region all the involved species absorb, and it is difficult to separate the absorption bands of the triplet states from that of the semireduced dye, but the absorption remaining after 30  $\mu\text{s}$  with  $\lambda_{\text{max}}$  ca. 700 nm can be assigned to the semireduced form of the dye [13]. The latter is formed when the deprotonated dye is quenched by a second molecule of the dendrimer by a sequential electron–proton transfer process. Similar behavior was observed for the other dendrimers, DAB-GO and PAMAM-G2.

Based on these observations the triplet quenching mechanism may be described by the reaction sequence shown in Scheme 2. In the scheme, the dendrimer quencher is represented by a tertiary amine structure. Initially a fast proton transfer equilibrium in the excited state, most likely involving a triplet exciplex, is established. This equilibrium is necessary in order to explain the downward curvature in the plots of the first-order decay rate constant vs. quencher concentration. Afterwards, the exciplex decays to the unprotonated form of the dye, as evidenced by the transient spectrum in Figs. 4 and 5, which in turn undergoes an electron transfer reaction with a second dendrimer molecule.

The last step is an electron transfer process followed by a fast in-cage proton transfer that leads to the radical in the alpha position of the amino groups of the dendrimers. This is postulated on the grounds of the demonstrated ability of the  $\text{SfH}^+$ –aliphatic amine system to initiate radical polymerization. In this case the active radical arises in the deprotonation of the amine radical cation produced in the electron transfer quenching of the triplet state of the dye.

According to Scheme 2, the observed first-order rate constant  $k_1$  for the decay of  ${}^3\text{SfH}^+$  can be analyzed by Eq. (2) [12,14] where  $[Q]$  stands for the quencher concentration. Values of  $k_1$  were determined by following the triplet decay at 820 nm:

$$k_1 = \frac{k_0 + k_d K_{\text{exc}} [Q]}{1 + K_{\text{exc}} [Q]} \quad (2)$$

The value of  $k_0$  was obtained to be  $7.2 \times 10^5 \text{ s}^{-1}$  from the decay of the triplet state in the absence of the quencher. From a non-linear least-squares analysis of the data, the equilibrium constant  $K_{\text{exc}}$  and the unimolecular rate constant for the decay of the exciplex  $k_d$ , can be obtained, and they are collected in Table 1. The solid lines in Fig. 2 represent the result of the fitting. It can be seen that while  $k_d$  remains practically constant in the order of  $1 \times 10^6 \text{ s}^{-1}$  the equilibrium constant changes two orders of magnitude. The

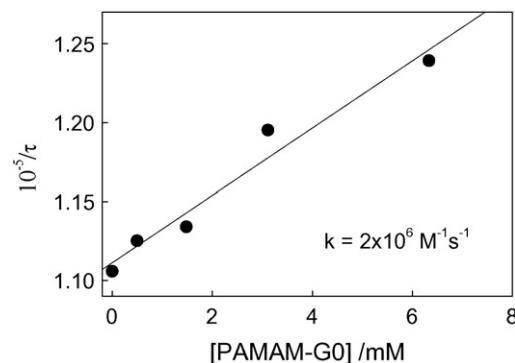


Fig. 7. Quenching of the deprotonated triplet,  ${}^3\text{Sf}$  by PAMAM-GO measured at 660 nm.

independence of  $k_d$  on the quencher structure is an indication that it corresponds to the decay of the exciplex to the free unprotonated triplet  ${}^3\text{S}$ , and not to the subsequent electron transfer reaction, since in this case a dependence with the electron donating capability should be expected, as it is found for the singlet quenching.

The kinetics of the last step was investigated by laser flash photolysis of the safranin-O–dendrimer system in the presence of NaOH 1 mM. By following the decay of the unprotonated triplet at 660 nm as a function of dendrimer concentration the rate constants for the electron transfer quenching of  ${}^3\text{Sf}$  could be determined. The quenching process in this case corresponds to an electron transfer process, and the rate constants are much lower (ca.  $1 \times 10^6 \text{ M}^{-1} \text{ s}^{-1}$ ) than those for singlet quenching due to the lower energy of the triplet state. In Fig. 7 a plot of the first-order rate constant for the decay of  ${}^3\text{Sf}$  as a function of PAMAM-GO concentration is shown. It can be seen that in this case a linear plot is obtained.

The values of  $K_{\text{exc}}$  bear a close relation with the number and basicity of the external amino groups in the quenchers. Thus, the higher value is for DAB which has four terminal primary amino groups with a  $\text{pK}_b$  4.15 [15], followed by PAMAM-G2 with 16 peripheral primary amines with a  $\text{pK}_b$  of 4.85 [16]. The trend is understood in terms of the basicity of the peripheral primary amino groups of the dendritic structure without participation of the interior tertiary groups. In an experimental and theoretical study of proton binding to PAMAM dendrimers, Niu et al. [16] concluded that interior amine groups have a smaller proton affinity compared to a single isolated amine group. TEA and BA have similar values  $K_{\text{exc}}$  lower than those of DAB and PAMAM-G2, but in agreement with the trend since they present only one proton acceptor site. The lowest values correspond to PAMAM-G0 and AEDA. In the case of PAMAM-G0 the value is one-fourth that of PAMAM-G2, as expected from the number of basic sites if it is accepted that they have similar proton affinity. In the case of AEDA the low value corresponds to a lower proton binding constant estimated by conductivity measurements.

The triplet quenching by TEOHA produces a linear plot for  $k_1$  vs. TEOHA concentration, with an apparent bimolecular quenching rate constant of  $3.8 \times 10^6 \text{ M}^{-1} \text{ s}^{-1}$ . This is due to the low basicity of this amine ( $\text{pK}_b = 6.24$ ) that changes the quenching mechanism to an electron transfer process, with a rate constant as expected for this type of reaction. On the other hand, for N,N-dimethylaniline a very poor base but a good electron donor, a linear plot is obtained, with a rate constant of  $5.2 \times 10^9 \text{ M}^{-1} \text{ s}^{-1}$ .

## 5. Conclusions

The quenching of the excited states of safranin by low generation dendrimers follows a complex mechanism, the nature of

which depends on the excited state involved. The singlet state quenching correlates with the number of external primary amino groups in the dendrimer, and in view of the deactivating effect of the amide moiety a direct electron transfer may be operating, although the intermediacy of an exciplex, albeit highly improbable in polar solvents, cannot be totally excluded. A proton transfer equilibrium mediates the triplet state quenching mechanism. Afterwards, a slower electron transfer process leads to the formation of the semireduced dye and probably a radical of the quencher, although not directly detected, as final species in the triplet quenching. The origin of the differences in the quenching mechanism of singlet and triplet states is not clear. It may be due to differences in the pK of the excited states, or the pre-eminence of the electron transfer reaction in the case of the singlet due to the higher energy of the state involved.

### Acknowledgments

Thanks are given to Consejo Nacional de Investigaciones Científicas y Técnicas (CONICET-PIP 5605), Agencia Nacional de Promoción Científica (ANPCYT-PICT 32351) and Universidad Nacional de Río Cuarto, Argentina, for financial support of this work. SGB and CMP hold a research position at CONICET. CAS thanks ANPCYT for a research fellowship.

### References

- [1] S. Svenson, D.A. Tomalia, Dendrimers in biomedical applications—reflections on the field, *Adv. Drug Deliv. Rev.* 57 (2005) 2106.
- [2] U. Boas, J.B. Christensen, P.M.H. Heegaard, *Dendrimers in Medicine and Biotechnology: New Molecular Tools*, RSC Publishing, London, 2006.
- [3] A.M. Chen, L.M. Santhakumaran, S.K. Nair, P.S. Amenta, T. Thomas, H.E. Huixin, T.J. Thomas, *Nanotechnology* 17 (2006) 5449; C.F.J. Faul, M. Antonietti, H.-P. Hentze, *Colloid Surf. A: Physicochem. Eng.* 212 (2003) 115.
- [4] M.A. Tasdelen, A.L. Demirel, Y. Yaggi, *Eur. Polym. J.* 43 (2007) 4423.
- [5] X. Jiang, W. Wang, H. Xua, J. Yin, *J. Photochem. Photobiol. A: Chem.* 181 (2006) 233.
- [6] C.M. Previtali, S.G. Bertolotti, M.G. Neumann, I.A. Pastre, A.M. Rufs, M.V. Encinas, *Macromolecules* 27 (1994) 7454.
- [7] M.V. Encinas, A.M. Rufs, M.G. Neumann, C.M. Previtali, *Polymer* 37 (1996) 1395.
- [8] M.L. Gómez, V. Avila, H.A. Montejano, C.M. Previtali, *Polymer* 44 (2003) 2875.
- [9] M.G. Neumann, I. Pastre, C.M. Previtali, *J. Photochem. Photobiol. A: Chem.* 61 (1991) 91.
- [10] M.V. Encinas, C.M. Previtali, S.G. Bertolotti, M.G. Neumann, *Photochem. Photobiol.* 62 (1995) 65.
- [11] M.V. Encinas, C.M. Previtali, M.H. Gehlen, M.G. Neumann, *J. Photochem. Photobiol. A: Chem.* 94 (1996) 237.
- [12] M.F. Broglia, S.G. Bertolotti, C.M. Previtali, *Photochem. Photobiol.* 83 (2007) 535.
- [13] S.N. Guha, J.P. Mittal, *J. Chem. Soc. Faraday Trans.* 93 (1997) 3647.
- [14] M.T. Yamaji, T. Tanaka, K. Suto, H. Shizuka, *Chem. Phys. Lett.* 261 (1996) 289; T. Kiyota, M. Yamaji, H. Shizuka, *J. Phys. Chem.* 100 (1996) 672 (and references therein).
- [15] V.A. Kabanov, A.B. Zevin, V.B. Rogacheva, Zh.G. Gulyaeva, M.F. Zansochova, J.G.H. Joosten, J. Brackman, *Macromolecules* 31 (1998) 5142.
- [16] Y. Niu, L. Sun, R.M. Crooks, *Macromolecules* 36 (2003) 5725.